

# Effects of Mandrel Angle on Hydrostatic Extrusion Process of Magnesium Alloy Tube

Zhao Mengjun, Wu Zhilin, Cai Hongming

Nanjing University of Science & Technology, Nanjing 210094, China

**Abstract:** The hydrostatic extrusion process of magnesium alloy AZ80 tube with different mandrel angles ( $90^\circ$ ;  $120^\circ$ ;  $150^\circ$ ) was simulated by the DEFORM-3D software with different extrusion speeds and initial billet temperatures. The simulated results show that the peak load of the extrusion process with big mandrel angle is obviously higher than that of the small angle and the inhomogeneity of billet velocity field is intensified with the increase of the mandrel angle.

**Key words:** hydrostatic extrusion; AZ80; mandrel angle

Hydrostatic extrusion is favorable for many refractory materials, which can obviously enhance its plasticity, decrease internal cracking, and makes microstructure of the extruded product homogeneous and mechanical properties good<sup>[1,2]</sup>. Till now, the hydrostatic extrusion technique has been extensively used in metal materials, composite materials, military materials and medical materials<sup>[3]</sup>. As shown in Fig.1, the key parts for the hydrostatic extrusion system mainly contain die, mandrel, ram, container, pressure medium and billet. The billet is placed inside the container, and has to be tapered to match the die geometry. The gap between the billet and the container is filled with the pressure medium which surrounds the billet and transforms the force on the billet. When the force becomes high enough, the billet is pressed through the die and the mandrel. During the process, the pressure medium is forced by its inherent pressure into the gap between the die and the billet where it acts as a lubricant effectively.

Presently, many academic achievements had been obtained, mainly including the effects of initial temperature on hydrostatic extrusion process, for example, J. Swiostek et al conducted research on AZ31, AZ61, AZ80, ZM21, ZK30 and ZE10 and acquired the lowest extrusion temperatures of those alloys<sup>[4]</sup>. Wang Rong, A. Y. Volkov et al extruded hydrostatic bars of magnesium alloy AZ31 and pure magnesium (99.98%) at room temperature<sup>[5,6]</sup>. In addition, Shaochun Wang,

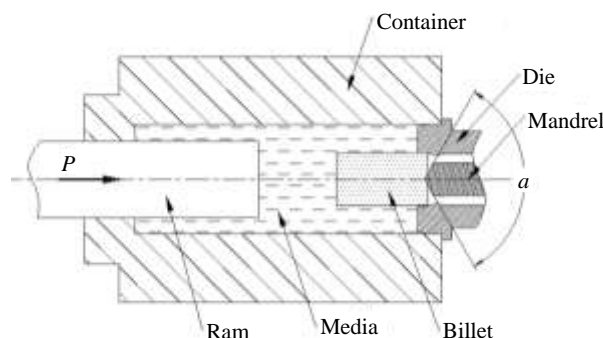


Fig.1 Principle of hydrostatic extrusion of tube

Zhilin Wu et al conducted researches on a warm extrusion technique for extrusion of magnesium alloys<sup>[7,8]</sup>. Zhao Zude studied the effects of extrusion ratio on loads<sup>[9]</sup>.

The above studies mostly centered on initial billet temperature, extrusion speed and ratio. However, there is few reports about effects of mandrel angle on hydrostatic extrusion process of magnesium alloy. In the present research, the effects of mandrel angle on extrusion process have been simulated and discussed.

## 1 Finite Element Simulations

Received date: May 25, 2016

Foundation item: National Science and Technology Major Project (2012ZX04010101)

Corresponding author: Wu Zhilin, Ph. D., Professor, Office of Science and Technology Research, Nanjing University of Science & Technology, Nanjing 210094, P. R. China, E-mail: wuruinan-1994@njjust.edu.cn

Copyright © 2017, Northwest Institute for Nonferrous Metal Research. Published by Elsevier BV. All rights reserved.

The geometry model was axisymmetric, of which 1/4 part was taken in the present research. The model mainly include ram, media, billet, mandrel, die and container, as shown in Fig.1 and Fig.2. Before simulation, the geometry model was meshed to 4-node tetrahedrons, of which side length of grids was 2 mm at the least and 4 mm at the most.

Billet is made of magnesium alloy AZ80 in the simulation<sup>[10]</sup>, with its physical properties shown in Table 1.

A constitutive equation<sup>[11]</sup> was adopted to describe the hot compression of magnesium alloy AZ80, as follows:

$$\dot{\epsilon} = 2.9 \times 10^9 [\sinh(0.0174\sigma)]^{6.905} \exp\left[-\frac{(154.6 \times 10^3)}{8.314T}\right]$$

The above equation was built on the experiments of the hot compression of AZ80, which were carried out on Gleeble-1500 thermal simulator at a strain rate of  $1 \times 10^{-3} \sim 20 \text{ s}^{-1}$  and temperature range of 200~500 °C. In the above equation, the parameter  $\sigma$  was determined by peak stress (MPa) for a given strain, and  $T$  denoted absolute temperature.

Friction stress between the billet, the die and the mandrel was determined by deformation temperature, lubricant condition, which is commonly complicated. For the simplified calculation, limit frictional state was adopted in the present research, that is, providing that friction reaches the shear yield limit of the corresponding deformation temperature and its distribution is uniform. Friction factor between the die and billet was 0.1, so did the factor between the mandrel and the billet. The heat transfer coefficient between the billet and the mandrel, the die and the billet is  $7.5 \text{ W}/(\text{m}^2 \text{ K})$ .

To analyze effects of the mandrel angle on extrusion loads, effective stress distribution and velocity field were simulated by DEFORM-3D software. Firstly, the mandrel angle was divided into three groups: 90°, 120° and 150°; Secondly, the simulation of the three mandrel angles were conducted with different extrusion speeds: 1, 10 and 50 mm/s, and constant initial billet temperature; At last, the simulation were conducted

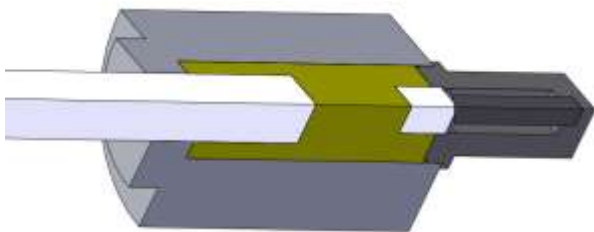


Fig.2 Geometry model of hydrostatic extrusion of tube

Table 1 Physical property parameters of material

$E/\text{GPa}$	$\nu$	$\alpha/\times 10^{-6} \text{ K}^{-1}$	$\lambda/\text{W} (\text{m K})^{-1}$
45	0.35	27.6	75.36

Note:  $E$  denotes elastic modulus;  $\nu$  denotes Poisson ratio;  $\alpha$  denotes expansion coefficient;  $\lambda$  denotes thermal conductivity; Test temperature is 573 K

again with different initial billet temperatures: 250, 150 and 90 °C. According to different initial billet temperatures of the billet and the extrusion speed, the simulations arranged in the present research are as follows:

- A90-T250-S1, A120-T250-S1, A150-T250-S1, (simulations with speed  $v=1 \text{ mm/s}$ );
- A90-T250-S10, A120-T250-S10, A150-T250-S10, (simulations with speed  $v=10 \text{ mm/s}$ );
- A90-T250-S50, A120-T250-S50, A150-T250-S50, (simulations with speed  $v=50 \text{ mm/s}$ );
- A90-T250-S10, A120-T250-S10, A150-T250-S10, (simulations with initial billet temperature  $T_0=250 \text{ °C}$ );
- A90-T150-S10, A120-T150-S10, A150-T150-S10, (simulations with initial billet temperature  $T_0=150 \text{ °C}$ );
- A90-T90-S10, A120-T90-S10, A150-T90-S10, (simulations with initial billet temperature  $T_0=90 \text{ °C}$ ).

## 2 Results and Discussion

The mandrel angle is set as 90°, 120° and 150°. The extrusion speed is set 1, 10 and 50 mm/s. Initial billet temperature is 250 °C. The effects of the mandrel angle on extrusion loads with different extrusion speeds are shown in Fig.3.

The effects of the mandrel angle on extrusion loads with different initial billet temperature are shown in Fig.3b, Fig.4a, 4b. The extrusion speed is set as 10 mm/s. Initial billet temperature is set as 250, 150 and 90 °C.

Different from the conventional extrusion method<sup>[12,13]</sup>, the hydrostatic extrusion loads in initial state for all simulations reaches their maximal values rapidly. The extrusion loads decrease with the increase of the mandrel angle slightly, since there is lack of filling process. Likewise, this law exists with different extrusion speeds and initial billet temperatures severally, as shown in Fig.3 and Fig.4. From Fig.3 and Fig.4, we can see that the extrusion loads is maximal with the mandrel angle 150°, and is nearly equal between 90° and 120°, which is the result of the comprehensive effect of friction stress on the mandrel end and deformation stress in billet.

The maximum effective stress appears on mandrel tip, as shown in Fig.5a, 5b, 5c. The maximum effective stress is 171 MPa with the mandrel angle 90°, 147 MPa with the mandrel angle 120° and 166 MPa with the mandrel angle 150°. Besides, the maximum effective stress distribution moves upward with the increase of extrusion speed, as shown in Fig.5d, 5e, 5f.

In addition, the results of simulation show that the billet velocity field is inhomogeneous in die exit, that is, the velocity is slow near the wall of die and mandrel. When the mandrel angle is 150°, this inhomogeneity is more outstanding; however, the velocity near side of the mandrel increases with increase of the mandrel angle and extrusion speed, as shown in Fig.6.

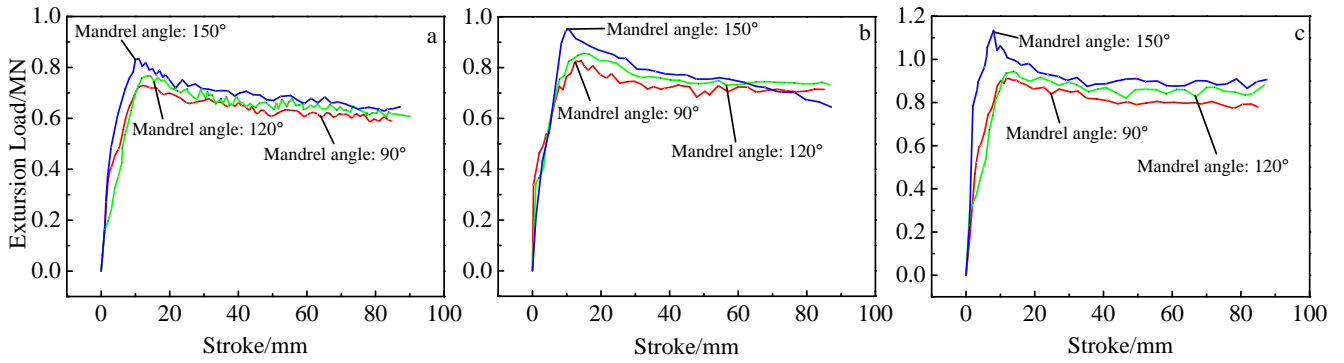


Fig.3 Effects of the mandrel angle on extrusion loads: (a)  $v=1$  mm/s,  $T_0=250$  °C, (b)  $v=10$  mm/s,  $T_0=250$  °C, and (c)  $v=50$  mm/s,  $T_0=250$  °C

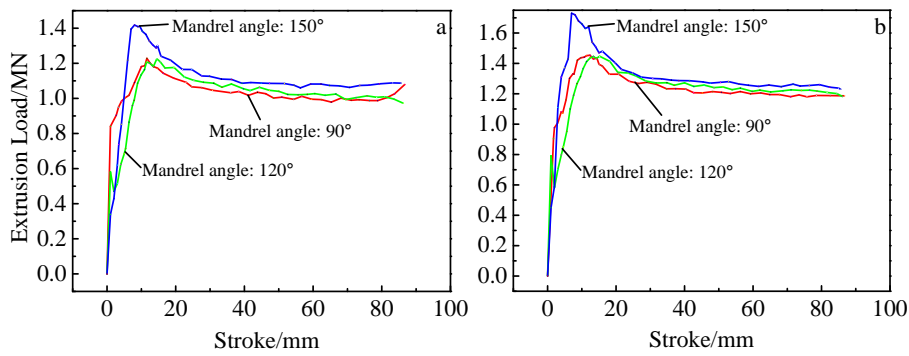


Fig.4 Effects of the mandrel angle on extrusion loads: (a)  $v=10$  mm/s,  $T_0=150$  °C and (b)  $v=10$  mm/s,  $T_0=90$  °C

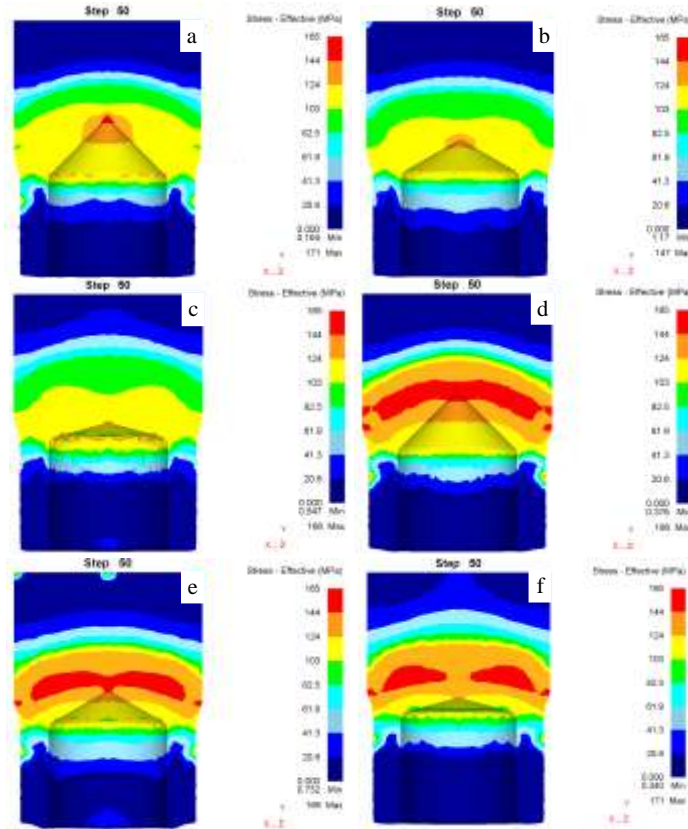


Fig.5 Effective stress distribution of the different mandrel angle: (a)  $\alpha=90^\circ$ ,  $v=1$  mm/s; (b)  $\alpha=120^\circ$ ,  $v=1$  mm/s; (c)  $\alpha=120^\circ$ ,  $v=1$  mm/s; (d)  $\alpha=90^\circ$ ,  $v=10$  mm/s; (e)  $\alpha=120^\circ$ ,  $v=10$  mm/s; (f)  $\alpha=150^\circ$ ,  $v=10$  mm/s

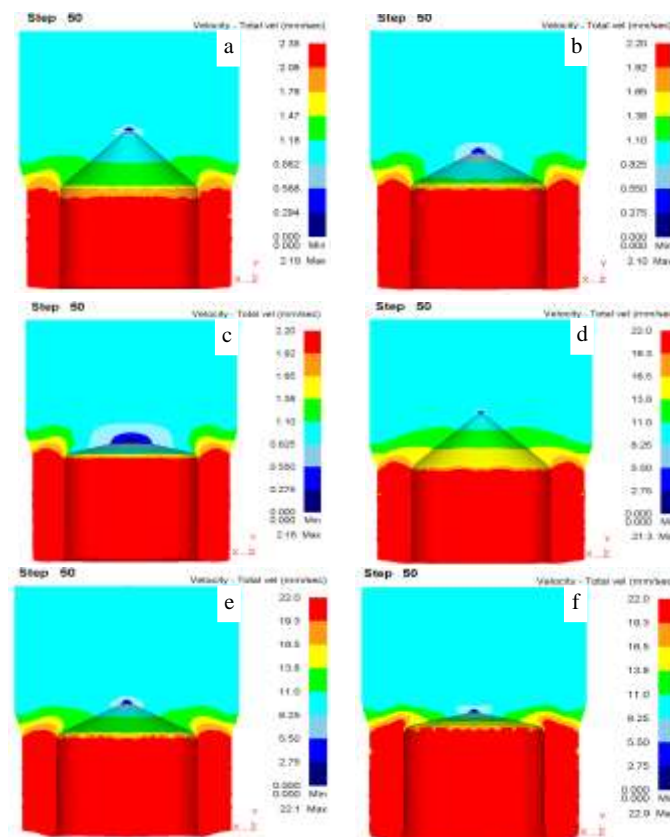


Fig.6 Billet flow field of the different mandrel angle: (a)  $\alpha=90^\circ$ ,  $v=1$  mm/s; (b)  $\alpha=120^\circ$ ,  $v=1$  mm/s; (c)  $\alpha=150^\circ$ ,  $v=1$  mm/s; (d)  $\alpha=90^\circ$ ,  $v=10$  mm/s; (e)  $\alpha=120^\circ$ ,  $v=10$  mm/s; (f)  $\alpha=150^\circ$ ,  $v=10$  mm/s

### 3 Conclusions

1) The load-stroke curve accords with conventional extrusion processes basically, but the loads reaches its peak value more rapidly in the hydrostatic extrusion process.

2) The extrusion load decreases with the increase of the mandrel angle slightly at the same extrusion speed and the initial billet temperature.

3) The effect of the mandrel angle on effective stress distribution is not obvious.

4) The billet flow field is inhomogeneous in die exit; besides, the flow velocity near the mandrel side increases with increase of the mandrel angle and extrusion speed.

### References

- 1 Wang Fuchi, Zhang Chaohui. *Hydrostatic Extrusion*[M]. Beijing: National Defense Industry Press, 2008 (in Chinese)
- 2 Bolen J, Yi S B, Letzig D et al. *Scripta Materialia*[J], 2005, 53(2): 259
- 3 Hu Jun, Yan L, Ren Z et al. *Hot Working Technology*[J], 2014, 43(15): 20 (in Chinese)
- 4 Swiostek J, Goken J, Letzig D et al. *Materials Science and Engineering A*[J], 2006, 424: 223
- 5 Wang Rong, Zhu Xiurong, Yang Bo et al. *J Cent South Univ, Science and Technology*[J], 2008, 39(2): 251
- 6 Volkov A Y, Kliukin I V. *Materials Science and Engineering A*[J], 2015, 627: 56
- 7 Wang Shaochun, Li Qiang, Zhang Guofeng et al. *Light Alloy Fabrication Technology*[J], 2008, 36(11): 34
- 8 Wu Zhilin, Wang Yujie, Yuan Renshu et al. *Hot Working Technology*[J], 2014, 43(11): 94 (in Chinese)
- 9 Zhao Zude, Wang Shaochun, Hu Chuankai et al. *China Mechanical Engineering*[J], 2008, 19(9): 1111
- 10 Chen Zhenghua. *Wrought Magnesium Alloys*[M]. Beijing: Chemical Industry Press, 2008 (in Chinese)
- 11 Zhou H T, Li Q B, Zhao Z K et al. *Materials Science and Engineering A*[J], 2010, 527(100): 2022
- 12 Cui Jianzhong, Wang Zhongtang, Zhao Genfa. *MACE 2011-Proceedings*[C]. New York: IEEE, 2011: 4317
- 13 Hwang Y, Chang Chengnan. *Procedia Engineering*[J], 2014, 81: 2249

## 模芯角度对镁合金管材静液挤压的影响

赵孟军, 吴志林, 蔡红明  
(南京理工大学, 江苏 南京 210094)

**摘要:** 通过 DEFORM-3D 软件模拟了不同的挤压速度与初始坯料温度条件下, 模芯的角度 ( $90^\circ$ ;  $120^\circ$ ;  $150^\circ$ ) 对管材静液挤压成形过程的影响。模拟结果显示, 静液挤压过程中大角度模芯的压力峰值明显高于小角度模芯的压力峰值, 同时随着模芯角度的增大管材的速度场分布不均性增加。

**关键词:** 静液挤压; AZ80; 模芯角度

---

作者简介: 赵孟军, 男, 1982 年生, 博士生, 南京理工大学机械工程学院, 江苏 南京 210094, E-mail: 511720141@qq.com